

Direct sampling of the Susskind–Glogower phase distributions

M. Dakna, L. Knöll, and D.–G. Welsch

Friedrich-Schiller-Universität Jena
Theoretisch-Physikalisches Institut
Max-Wien Platz 1, D-07743 Jena, Germany

Abstract

Coarse-grained phase distributions are introduced that approximate to the Susskind–Glogower cosine and sine phase distributions. The integral relations between the phase distributions and the phase-parametrized field-strength distributions observable in balanced homodyning are derived and the integral kernels are analyzed. It is shown that the phase distributions can be directly sampled from the field-strength distributions which offers the possibility of measuring the Susskind–Glogower cosine and sine phase distributions with sufficiently well accuracy. Numerical simulations are performed to demonstrate the applicability of the method.

1 Introduction

Although the problem of defining and measuring quantum mechanical phases of radiation-field modes has been discussed for a long time, there has been no unified approach to the phase problem so far [1]. The reason is that there is no “good” (i.e., self-adjoint) phase operator in the Hilbert space. The difficulties obviously arise from the boundedness of the eigenvalue spectrum of the photon-number operator, which is the canonically conjugate of the phase operator.

One way to overcome the difficulties was proposed by Susskind and Glogower [2] who used the non-Hermitian exponential phase operator and its adjoint in order to define two Hermitian operators. From the analogy between them and classical trigonometric functions the two operators are also referred to as cosine and sine phase operators. In particular in the classical limit they exactly correspond to the cosine and the sine of the phase. Since the cosine and sine phase operators are self-adjoint, their eigenstates can be used to define proper probability distributions for observing the cosine and sine phases. However, these distributions cannot be measured, in general, simultaneously and do therefore not uniquely characterize the phase of the quantum state of a mode. This is obviously the price to pay for introducing self-adjoint operators and keeping the concept of quantum mechanical probabilities.

In the classical limit the difference between the cosine and sine phase distributions vanishes. In particular, in classical optics the phase difference between two radiation-field modes can always be determined by simultaneously measuring the cosine and sine of the phase difference in interference experiments. Inspired by such kinds of measurements, Noh, Fougères, and Mandel [3] introduced an operational approach to the cosine and sine phase operators. As expected, for classical fields the corresponding phase distributions agree with the quantum mechanical Susskind–Glogower (SG) phase distributions, but for quantum fields they may be quite different from each other.

A powerful interferometric method for determining phase-sensitive properties of optical fields has been balanced homodyne detection. It is well known that from the data recorded in a succession of measurements the quantum state of a signal mode can be obtained, as was first demonstrated experimentally by Smithey, Beck, Faridani, and Raymer using optical homodyne tomography [4]. Knowing the quantum state (in terms of, e.g., the density matrix in a chosen basis), the quantum phase statistics can be calculated [5]. In the present paper we show that the SG cosine and sine phase distributions can be measured more directly by sampling them from the recorded data [6].

The approach is based on the introduction of parametrized cosine and sine phase distributions that are defined on the basis of appropriately coarse-

grained SG cosine and sine quantum states. So, the parametrized distributions can be regarded as smoothed SG cosine and sine phase distributions that reflect the exact statistics in a coarse-graining approximation. The accuracy is determined by the parameter that defines the phase coarse-graining interval. In particular, the parametrized distributions tend to the exact ones when the coarse-graining parameter approaches zero.

The advantage of the method is that for any non-zero value of the parameter the coarse-grained sine and cosine phase distributions can be directly sampled from the recorded data in balanced homodyning. Hence, choosing the coarse-graining interval small enough, the exact distributions can be measured with sufficiently well accuracy. Since in balanced homodyning the observed difference-count statistics is (for chosen phase parameters of the apparatus) a scaled field strength distribution of the signal mode, the sampling function needed is given by the kernel in the integral relation between the parametrized cosine and sine phase distributions and the phase-parametrized field-strength distributions.

The paper is organized as follows. In Sec. 2 coarse-grained cosine and sine phase distributions are introduced. Section 3 is devoted to the relations of the phase distributions to the field-strength distributions and the calculation of the cosine and sine phase sampling functions. In the Sec. 4 results of computer simulations of measurements of the cosine and sine phase distributions for a squeezed vacuum state are presented, and a summary and some concluding remarks are given in Sec. 5.

2 Coarse-grained cosine and sine phase distributions

Using the exponential phase operator

$$\hat{E} = \sum_{n=0}^{\infty} |n\rangle\langle n+1| \quad (1)$$

($\hat{n}|n\rangle = n|n\rangle$, $\hat{n} = \hat{a}^\dagger\hat{a}$, $[\hat{a}, \hat{a}^\dagger] = 1$), Susskind and Glogower [2] introduced the Hermitian cosine and sine operators

$$\hat{C} = \frac{1}{2}(\hat{E} + \hat{E}^\dagger) \quad (2)$$

and

$$\hat{S} = -\frac{1}{2}i(\hat{E} - \hat{E}^\dagger), \quad (3)$$

respectively, which satisfy the eigenvalue equations

$$\hat{C}|\cos\phi\rangle = \cos\phi|\cos\phi\rangle \quad (4)$$

($0 \leq \phi \leq \pi$) and

$$\hat{S}|\sin\phi\rangle = \sin\phi|\sin\phi\rangle \quad (5)$$

$(-\pi/2 \leq \phi \leq \pi/2)$. The SG cosine and sine phase states $|\cos \phi\rangle$ and $|\sin \phi\rangle$, respectively, form orthonormal and complete sets in the Hilbert space, that is to say,

$$\langle \cos \phi | \cos \phi' \rangle = \delta(\phi - \phi'), \quad (6)$$

$$\int_0^\pi d\phi |\cos \phi\rangle \langle \cos \phi| = \hat{I} \quad (7)$$

and

$$\langle \sin \phi | \sin \phi' \rangle = \delta(\phi - \phi'), \quad (8)$$

$$\int_{-\pi/2}^{\pi/2} d\phi |\sin \phi\rangle \langle \sin \phi| = \hat{I}. \quad (9)$$

In order to give a unified approach to the states, let us consider the ψ -parametrized Hermitian operator

$$\hat{C}(\psi) = \frac{1}{2}(\hat{E}e^{-i\psi} + \hat{E}^\dagger e^{i\psi}). \quad (10)$$

Recalling Eq. (1), $\hat{C}(\psi)$ is easily proved to satisfy the eigenvalue equation

$$\hat{C}(\psi) |\Phi, \psi\rangle = \cos \Phi |\Phi, \psi\rangle, \quad (11)$$

where

$$|\Phi, \psi\rangle = \sqrt{\frac{2}{\pi}} \sum_n e^{in\psi} \sin[(n+1)\Phi] |n\rangle. \quad (12)$$

Note that $|- \Phi, \psi\rangle = -|\Phi, \psi\rangle$ and $|\Phi + \pi, \psi\rangle = |\Phi, \psi + \pi\rangle$. For chosen ψ the states $|\Phi, \psi\rangle$, $0 \leq \Phi \leq \pi$, form an orthonormal complete basis. The SG cosine and sine phase states in Eqs. (4) and (5), respectively, can be obtained by appropriately specifying the states $|\Phi, \psi\rangle$,

$$|\cos \phi\rangle = |\Phi = \phi, \psi = 0\rangle, \quad (13)$$

$$|\sin \phi\rangle = |\Phi = \frac{1}{2}\pi - \phi, \psi = \frac{1}{2}\pi\rangle. \quad (14)$$

With regard to measurements, we now introduce coarse-grained states as

$$|\Phi, \psi, \epsilon\rangle = \frac{1}{\sqrt{\epsilon}} \int_{\Phi-\epsilon/2}^{\Phi+\epsilon/2} d\Phi' |\Phi', \psi\rangle. \quad (15)$$

Using Eq. (12), the states $|\Phi, \psi, \epsilon\rangle$ can be given by

$$|\Phi, \psi, \epsilon\rangle = \sqrt{\frac{2\epsilon}{\pi}} \sum_n e^{in\psi} \sin[(n+1)\Phi] \text{sinc}[(n+1)\epsilon/2] |n\rangle \quad (16)$$

($\text{sinc } x = \sin x/x$). They are normalized to unity,

$$\langle \Phi, \psi, \epsilon | \Phi, \psi, \epsilon \rangle = 1, \quad (17)$$

and tend to the exact states $|\Phi, \psi\rangle$ as ϵ approaches zero,

$$\lim_{\epsilon \rightarrow 0} \frac{1}{\sqrt{\epsilon}} |\Phi, \psi, \epsilon\rangle = |\Phi, \psi\rangle. \quad (18)$$

The coarse-grained cosine and sine phase states, respectively, are obtained as $|\cos \phi, \epsilon\rangle = |\Phi = \phi, \psi = 0, \epsilon\rangle$ and $|\sin \phi, \epsilon\rangle = |\Phi = \frac{1}{2}\pi - \phi, \psi = \frac{1}{2}\pi, \epsilon\rangle$ [cf. Eqs. (13), (14), and (15)]. According to Eq. (18), they approach the exact SG cosine and sine phase states in the limit when $\epsilon \rightarrow 0$.

The states $|\Phi, \psi, \epsilon\rangle$ can be used to define parametrized phase distributions of a radiation-field mode via their overlaps with the quantum state $\hat{\rho}$ of the mode,

$$p(\Phi, \psi, \epsilon) = N^{-1}(\psi, \epsilon) \langle \Phi, \psi, \epsilon | \hat{\rho} | \Phi, \psi, \epsilon \rangle, \quad (19)$$

where the normalization factor

$$N(\psi, \epsilon) = \int_0^\pi d\Phi \langle \Phi, \psi, \epsilon | \hat{\rho} | \Phi, \psi, \epsilon \rangle \quad (20)$$

has been introduced. Note that $p(\Phi, \psi, \epsilon) \rightarrow p(\Phi, \phi) \equiv \langle \Phi, \psi | \hat{\rho} | \Phi, \psi \rangle$ when $\epsilon \rightarrow 0$. In particular, the coarse-grained cosine and sine phase state distributions $p_c(\phi, \epsilon)$ and $p_s(\phi, \epsilon)$ are given by

$$p_c(\phi, \epsilon) = p(\Phi = \phi, \psi = 0, \epsilon), \quad (21)$$

$$p_s(\phi, \epsilon) = p\left(\Phi = \frac{1}{2}\pi - \phi, \psi = \frac{1}{2}\pi, \epsilon\right) \quad (22)$$

[$p_c(\phi) \equiv \langle \cos \phi | \hat{\rho} | \cos \phi \rangle = \lim_{\epsilon \rightarrow 0} p_c(\phi, \epsilon)$, $p_s(\phi) \equiv \langle \sin \phi | \hat{\rho} | \sin \phi \rangle = \lim_{\epsilon \rightarrow 0} p_s(\phi, \epsilon)$]. The smaller the value of ϵ becomes the better the coarse-grained distributions approximate to the exact ones. In Figs. 1– 2 plots of $p_c(\phi, \epsilon)$ and $p_s(\phi, \epsilon)$ for various values of ϵ are shown for a mode prepared in a coherent state. We see that with increasing value of the mean number of photons the value of ϵ must be decreased in order to obtain the coarse-grained distributions comparably close to the exact ones. This is of course a reflection of the fact that with decreasing value of ϵ the value of the (effective) cut-off photon number in the expansion (16) is increased.

3 Relations to the phase-parametrized field-strength distributions

When we let $\epsilon = 0$, then Eq. (16) reduces, after multiplication by $\epsilon^{-1/2}$, to the expansion in the photon-number basis of the exact states $|\Phi, \psi\rangle$. All the photon-number states are seen to contribute to the exact states with comparable weight, which prevents one from directly sampling the exact distributions from the difference-count statistics recorded in balanced homodyning. The advantage of the coarse-grained distributions is that they can

be directly sampled from the recorded data. Since for sufficiently small values of the coarse-graining parameter the measured distributions approximate to the exact distributions with desired accuracy, the method enables us to asymptotically measure the exact distributions.

As already mentioned, the difference-count statistics recorded in balanced homodyning represents the statistics of a scaled field strength of the signal mode,

$$\hat{F}(\varphi) = |F|(\hat{a}e^{-i\varphi} + \hat{a}^\dagger e^{i\varphi}), \quad (23)$$

where the phase φ is determined by the chosen phase parameters of the apparatus (see, e.g., [7]). The desired sampling functions can be therefore obtained from the integral relations between the coarse-grained phase distributions $p(\Phi, \psi, \epsilon)$ and the phase-parametrized field-strength distributions of the signal field,

$$p(\mathcal{F}, \varphi) = \langle \mathcal{F}, \varphi | \hat{\rho} | \mathcal{F}, \varphi \rangle, \quad (24)$$

$|\mathcal{F}, \varphi\rangle$ being the eigenvectors of $\hat{F}(\varphi)$ (for details, see [7, 8]). For this purpose we note that the single-mode density operator can be expanded as [9, 10, 11, 12]

$$\hat{\rho} = \int_0^\pi d\varphi \int_{-\infty}^\infty d\mathcal{F} p(\mathcal{F}, \varphi; s) \hat{K}(\mathcal{F}, \varphi; -s), \quad (25)$$

where the smeared field-strength distributions $p(\mathcal{F}, \varphi; s)$, $s = 1 - \eta^{-1}$, have been introduced which are measured in non perfect detection, i.e., when the detection efficiency η is less than unity (see, e.g., [7]). The operator integral kernel $\hat{K}(\mathcal{F}, \varphi; -s)$ in Eq. (25) is given by

$$\hat{K}(\mathcal{F}, \varphi; -s) = \frac{|F|^2}{\pi} \int_{-\infty}^\infty dy |y| \exp\left\{iy \left[\hat{F}(\varphi) - \mathcal{F}\right] - \frac{1}{2}sy^2|F|^2\right\}. \quad (26)$$

Using Eq. (25), from Eq. (19) we easily find that $p(\Phi, \psi, \epsilon)$ can be related to $p(\mathcal{F}, \varphi; s)$ as

$$p(\Phi, \psi, \epsilon) = N^{-1}(\psi, \epsilon) \int_0^\pi d\varphi \int_{-\infty}^\infty d\mathcal{F} p(\mathcal{F}, \varphi; s) K_\epsilon(\Phi, \psi, \mathcal{F}, \varphi; s), \quad (27)$$

where

$$K_\epsilon(\Phi, \psi, \mathcal{F}, \varphi; s) = \langle \Phi, \psi, \epsilon | \hat{K}(\mathcal{F}, \varphi; -s) | \Phi, \psi, \epsilon \rangle. \quad (28)$$

Equation (27) can be regarded as the basic equation for direct sampling of the phase distributions $p(\Phi, \psi, \epsilon)$ from the difference-count statistics in balanced homodyning, where the integral kernel play the role of the sampling function. In order to calculate them, we substitute in Eq. (28) for $|\Phi, \psi, \epsilon\rangle$ the expansion Eq. (16), and we derive

$$K_\epsilon(\Phi, \psi, \mathcal{F}, \varphi; s) = \frac{2\epsilon}{\pi} \sum_{n=0}^\infty \sum_{m=0}^\infty \left\{ f_{nm}(x; s) \exp[i(n-m)(\varphi - \psi)] \right. \\ \left. \times \sin[(n+1)\Phi] \sin[(m+1)\Phi] \text{sinc}[(n+1)\epsilon/2] \text{sinc}[(m+1)\epsilon/2] \right\}, \quad (29)$$

where the function $f_{nm}(x; s)$, $x = \mathcal{F}/(\sqrt{2}|F|)$, is closely related to the sampling function

$$\langle n|\hat{K}(\mathcal{F}, \varphi; -s)|m\rangle = f_{nm}(x; s) \exp[i(n-m)\varphi] \quad (30)$$

for measuring the signal-mode density matrix in the photon-number basis [11, 12]. From inspection of Eqs. (26) and (29) we see that the symmetry relations

$$K_\epsilon(\Phi, \psi, \mathcal{F}, \varphi + \pi; s) = K_\epsilon(\Phi, \psi, -\mathcal{F}, \varphi; s), \quad (31)$$

$$K_\epsilon(\Phi, \psi, \mathcal{F}, \varphi + \pi; s) = K_\epsilon(\Phi - \pi, \psi, \mathcal{F}, \varphi; s), \quad (32)$$

$$K_\epsilon(-\Phi, \psi, \mathcal{F}, \varphi; s) = K_\epsilon(\Phi, \psi, \mathcal{F}, \varphi; s), \quad (33)$$

$$K_\epsilon(\Phi, -\psi, \mathcal{F}, -\varphi; s) = K_\epsilon(\Phi, \psi, \mathcal{F}, \varphi; s), \quad (34)$$

$$K_\epsilon(\Phi, \psi, \mathcal{F}, \varphi; s) = K_\epsilon(\Phi, 0, \mathcal{F}, \varphi - \psi; s) \quad (35)$$

are valid. Hence knowing the function

$$K_\epsilon(\Phi, \mathcal{F}, \varphi; s) \equiv K_\epsilon(\Phi, \psi = 0, \mathcal{F}, \varphi; s), \quad (36)$$

with $\Phi, \varphi \in (\pi/2)$ -intervals, the function $K_\epsilon(\Phi, \psi, \mathcal{F}, \varphi; s)$ is known for all values of Φ, ψ , and φ . In particular, the functions $K_\epsilon^c(\phi, \mathcal{F}, \varphi; s)$ and $K_\epsilon^s(\phi, \mathcal{F}, \varphi; s)$, respectively, that are required in order to relate the cosine and sine phase states distributions $p_c(\phi, \epsilon)$ and $p_s(\phi, \epsilon)$ to the field-strength distributions are given by

$$K_\epsilon^c(\phi, \mathcal{F}, \varphi; s) = K_\epsilon(\Phi = \phi, \mathcal{F}, \varphi; s), \quad (37)$$

$$K_\epsilon^s(\phi, \mathcal{F}, \varphi; s) = K_\epsilon(\Phi = \phi - \frac{1}{2}\pi, \mathcal{F}, \varphi - \frac{1}{2}\pi; s). \quad (38)$$

4 Direct sampling of the Susskind-Glogower phase distributions

The function $f_{nm}(x; s)$ in the series expansion (29) of the sampling function $K_\epsilon(\Phi, \mathcal{F}, \varphi; s)$, Eq. (36), has been studied in a number of papers and different algorithms for numerical calculations have been discussed (see [13, 14] and references therein). For the sake of transparency let us restrict attention to perfect detection ($\eta = 1$ and hence $s = 1 - \eta^{-1} = 0$). In this case, $f_{nm}(x) \equiv f_{nm}(x, s=0)$ can be written as

$$f_{nm}(x) = \frac{d}{dx} [\psi_n(x)\phi_m(x)] \quad \text{if } m \geq n \quad (39)$$

[$f_{nm}(x) = f_{mn}(x)$ if $m < n$], where $\psi_n(x)$ and $\phi_m(x)$, respectively, are the regular (normalizable) and irregular (unnormalizable) solutions of the energy eigenvalue equation of the harmonic oscillator for the n th eigenvalue [13, 14]. The asymptotic behaviour of $f_{nm}(x)$ for large values of n and m can be found

using the semiclassical (WKB) approximation. For the argument x within the classical allowed region $|x| < a_n \equiv (2n + 1)^{\frac{1}{2}}$ the function $f_{nm}(x)$ ($m \geq n$) becomes [14]

$$f_{nm}(x) \sim \frac{2}{\pi} (p_n p_m)^{-\frac{1}{2}} \left[p_m \cos\left(S_n + \frac{1}{4}\pi\right) \cos\left(S_m + \frac{1}{4}\pi\right) - p_n \sin\left(S_n + \frac{1}{4}\pi\right) \sin\left(S_m + \frac{1}{4}\pi\right) \right], \quad (40)$$

where

$$p_n(x) = \left(2n + 1 - x^2\right)^{\frac{1}{2}} \quad (41)$$

denotes the classical momentum and

$$S_n(x) = \int_{a_n}^x dx' p_n(x') \quad (42)$$

is the time-independent part of the classical action.

For proving the convergence of the series expansion of $K(\Phi, \mathcal{F}, \varphi; s=0)$, it is sufficient to substitute in Eq. (29) for $f_{nm}(x; s=0)$ the semiclassical expression (40). For $x/a_n \rightarrow 0$ the functions $p_n(x)$ and $S_n(x)$ in Eq. (40) behave like $n^{1/2}$ and $-(n + \frac{1}{2})\pi/2$, respectively, so that $(p_m(x)/p_n(x))^{\frac{1}{2}} \sim (m/n)^{\frac{1}{4}}$ and $\cos[S_n(x) + \pi/4] \sim \cos(n\pi/2)$, $\sin[S_n(x) + \pi/4] \sim -\sin(n\pi/2)$. Hence for any $\epsilon > 0$ the series expansion is expected to exist, because of the factor $(nm)^{-1}$ that arises from the sinc-functions. Results of numerical calculations of $K(\Phi, \mathcal{F}, \varphi; s=0)$ are shown in Fig. 3. It should be noted that $K(\Phi, \mathcal{F}, \varphi; s)$ separately depends on the two phases Φ and φ , whereas the sampling function for the London phase state distribution only depends on the difference phase [6].

In order to demonstrate the feasibility of direct sampling of the SG cosine and sine phase state distributions from the recorded difference count statistics in balanced homodyning, we have performed computer simulations of measurements of the phase-parametrized field-strength distributions $p(\mathcal{F}, \varphi)$ on an equidistant grid of points $\{\mathcal{F}_i, \varphi_j\}$. We have assumed that in the experiments the signal mode to be detected is prepared in a squeezed vacuum state

$$|\Psi\rangle = \exp\left\{-\frac{1}{2} \left[\xi(\hat{a}^\dagger)^2 - \xi^* \hat{a}^2\right]\right\} |0\rangle. \quad (43)$$

In particular, we have assumed that $10^4 \times 30$ events are recorded. From the results shown in Fig. 4 we see that the sampled distributions are in good agreement with the theoretical predictions. Their deviations from the exact distributions obviously result from the middle observational level chosen. Nevertheless, the accuracy is seen to be sufficient in order to detect the typical features of the exact distributions. From Eqs. (12) [together with Eqs.(13) and (14)] and (43) we easily see that the cosine and sine phase state distributions of the ordinary vacuum ($\xi = 0$) are given by $|\langle 0 | \cos \phi \rangle|^2 = (2/\pi) \sin^2 \phi$ and $|\langle 0 | \sin \phi \rangle|^2 = (2\pi)^{-1} \cos^2 \phi$, respectively. In this case the

cosine phase state distribution has a broad maximum at $\phi = \pi/2$, whereas the sine phase state distribution has a broad maximum at $\phi = 0$. When the value of ξ is increased ($\xi > 0$), the “vacuum noise circle” centred at the origin of co-ordinates in the (complex) α phase space is squeezed to an ellipse with the small semi-axis parallel to the real axis [15]. Hence, the cosine phase distribution is expected to become more sharply peaked at $\phi = \pi/2$. Accordingly, the sine phase state distribution is expected to show a double-peak structure, with the maxima close to $\phi = \pm\pi/2$ and the minimum at $\phi = 0$.

5 Summary and conclusions

In the paper we have studied the problem of measuring the SG cosine and sine phase state distributions in balanced homodyne detection. We have shown that they can be directly sampled, in a coarse-graining approximation, from the recorded difference-count statistics with sufficiently well accuracy. The accuracy is determined by the interval of field strengths used for “probing” the phase statistics of the signal-mode under consideration. With decreasing coarse-graining parameter, this interval is increased and the accuracy is increased as well.

It is worth noting that the SG cosine and sine phase state distributions can be regarded as special cases of ψ -parametrized phase state distributions. The latter are based on ψ -parametrized phase states that for $\psi = 0$ and $\psi = \frac{1}{2}\pi$ reduce to the cosine and sine phase states, respectively. Accordingly, the sampling functions for the cosine and sine phase state distributions can be obtained by specifying the sampling function for the ψ -parametrized phase distributions. Their integral relation to the field-strength distributions reveal that the sampling function exhibits a number of symmetry properties that can advantageously be used in calculations.

We have calculated the sampling function using an expansion in terms of the matrix elements of the corresponding operator integral kernel in the Fock basis. These matrix elements, which are the sampling functions required for measuring the signal-mode density matrix in the Fock basis, can be calculated applying the algorithm developed in [14]. In this way, the sampling function can be obtained for any (non-zero) coarse-graining parameter.

In order to give an example, we have performed computer simulations of measurements of the cosine and sine phase state distributions at a middle observational level (i.e., for a not extremely small coarse-graining parameter and a realistic grid of sampling points). Assuming that the signal mode is prepared in a squeezed vacuum state, the measured cosine and sine phase state distributions have been found to show the typical features of the exact distributions. Apart from the maxima and minima indicating the regions of nonclassical noise reduction and enhancement, respectively, qualitatively dif-

ferent shapings of the two distributions are observed which also demonstrate the quantum character of the state of the signal mode. It should be pointed out that the different shapings reflect the fact that for quantum states the (noncommuting) quantities cosine and sine cannot be related to a common phase. This effect is of course not observed in the London state phase distribution. Clearly, the introduction of a phase that cannot be related to a Hermitian operator is the price that is to be paid for a common phase.

6 Acknowledgements

This work was supported by the Deutsche Forschungsgemeinschaft. We would like to thank T. Opatrný and U. Leonhardt for discussions.

References

- [1] R. Lynch, Phys. Rep. **256**, 367 (1995).
- [2] L. Susskind and J. Glogower, Physics **1**, 49 (1964); P. Carruthers and M.M. Nieto, Phys. Rev. Lett. **14**, 387 (1965), Rev. Mod. Phys. **40**, 411 (1968).
- [3] J.W. Noh, A. Fougères, and L. Mandel, Phys. Rev. Lett. **67**, 1426 (1991), ibid. **71**, 2579 (1993), Phys. Rev. A **45**, 424 (1992), ibid. **46**, 2840 (1992), **47**, 4535, 4541 (1993).
- [4] D.T. Smithey, M. Beck, A. Faridani, and M.G. Raymer, Phys. Rev. Lett. **70**, 1244 (1993); D.T. Smithey, M. Beck, J. Cooper, M.G. Raymer, and A. Faridani, Physica Scripta T**48**, 35 (1993).
- [5] M. Beck, D.T. Smithey, and M.G. Raymer, Phys. Rev. A **48**, R890 (1993); D.T. Smithey, M. Beck, J. Cooper, and M.G. Raymer, Phys. Rev. A **48**, 3159 (1993).
- [6] For direct sampling of the London phase state distribution, see M. Dakna, L. Knöll, and D.-G. Welsch, quant-ph/9603027 (1996); Proceedings of the Fourth Central-European Workshop on Quantum Optics, Budmerice, 1996 (to be published in acta phys. slovac).
- [7] W. Vogel and D.-G. Welsch, *Lectures on Quantum Optics* (Akademie-Verlag, Berlin, 1994).
- [8] M. Schubert and W. Vogel, Phys. Lett. **68A**, 321 (1978).
- [9] K.E. Cahill and R. Glauber, Phys. Rev. **177**, 1857 (1969).
- [10] K. Vogel and H. Risken, Phys. Rev. A **40**, 2847 (1989).

- [11] G.M. D'Ariano, *Quantum Semiclass. Opt.* **7**, 693, (1995).
- [12] U. Leonhardt, H. Paul, and G.M. D'Ariano, *Phys. Rev. A* **52**, 4899 (1995).
- [13] Th. Richter, *Phys. Lett.* **211A**, 327 (1996).
- [14] U. Leonhardt, M. Munroe, T. Kiss, M. G. Raymer, and Th. Richter, *Opt. Commun.*, to be published.
- [15] R. Loudon and P.L. Knight, *J. Mod. Opt.* **34**, 709 (1987).

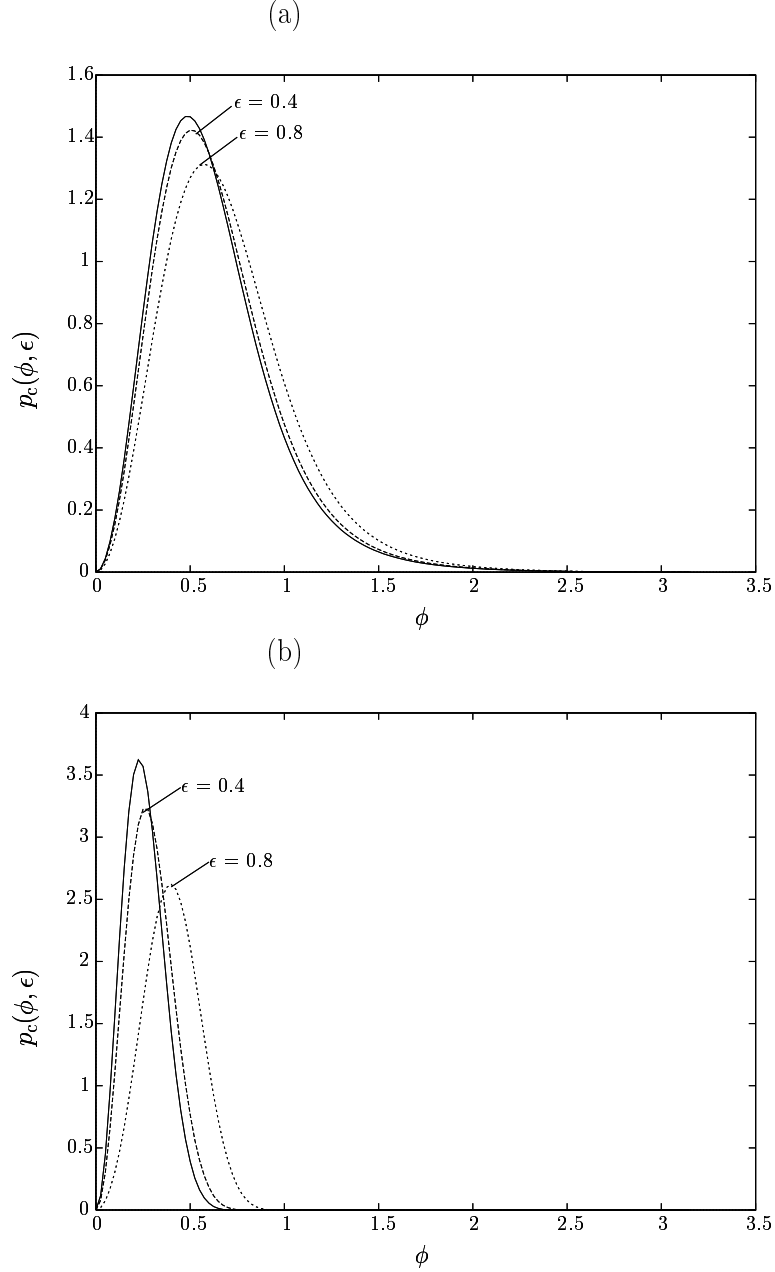


Figure 1: The coarse-grained cosine phase state distributions of a mode prepared in a coherent state $|\alpha\rangle$ with $\langle \hat{n} \rangle = 1$ ($\alpha = 1$) (a) and $\langle \hat{n} \rangle = 2$ ($\alpha = \sqrt{2}$) (b) are shown for $\epsilon = 0.4$ (dashed lines) and $\epsilon = 0.8$ (dotted lines). For comparison, the exact distributions that are observed in the limit $\epsilon \rightarrow 0$ are also shown (solid lines).

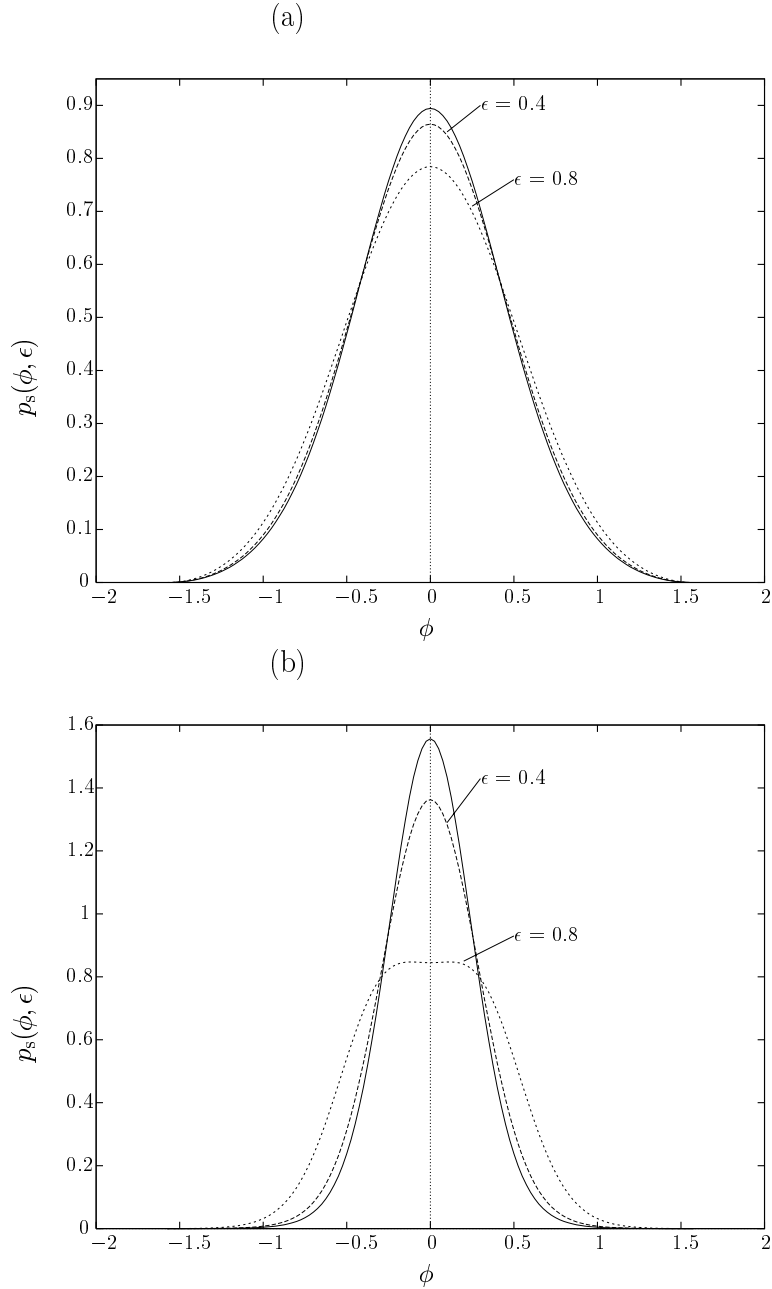


Figure 2: The coarse-grained sine phase state distributions of a mode prepared in a coherent state $|\alpha\rangle$ with $\langle\hat{n}\rangle = 1$ ($\alpha = 1$) (a) and $\langle\hat{n}\rangle = 2$ ($\alpha = \sqrt{2}$) (b) are shown for $\epsilon = 0.4$ (dashed lines) and $\epsilon = 0.8$ (dotted lines). For comparison, the exact distributions that are observed in the limit $\epsilon \rightarrow 0$ are also shown (solid lines).

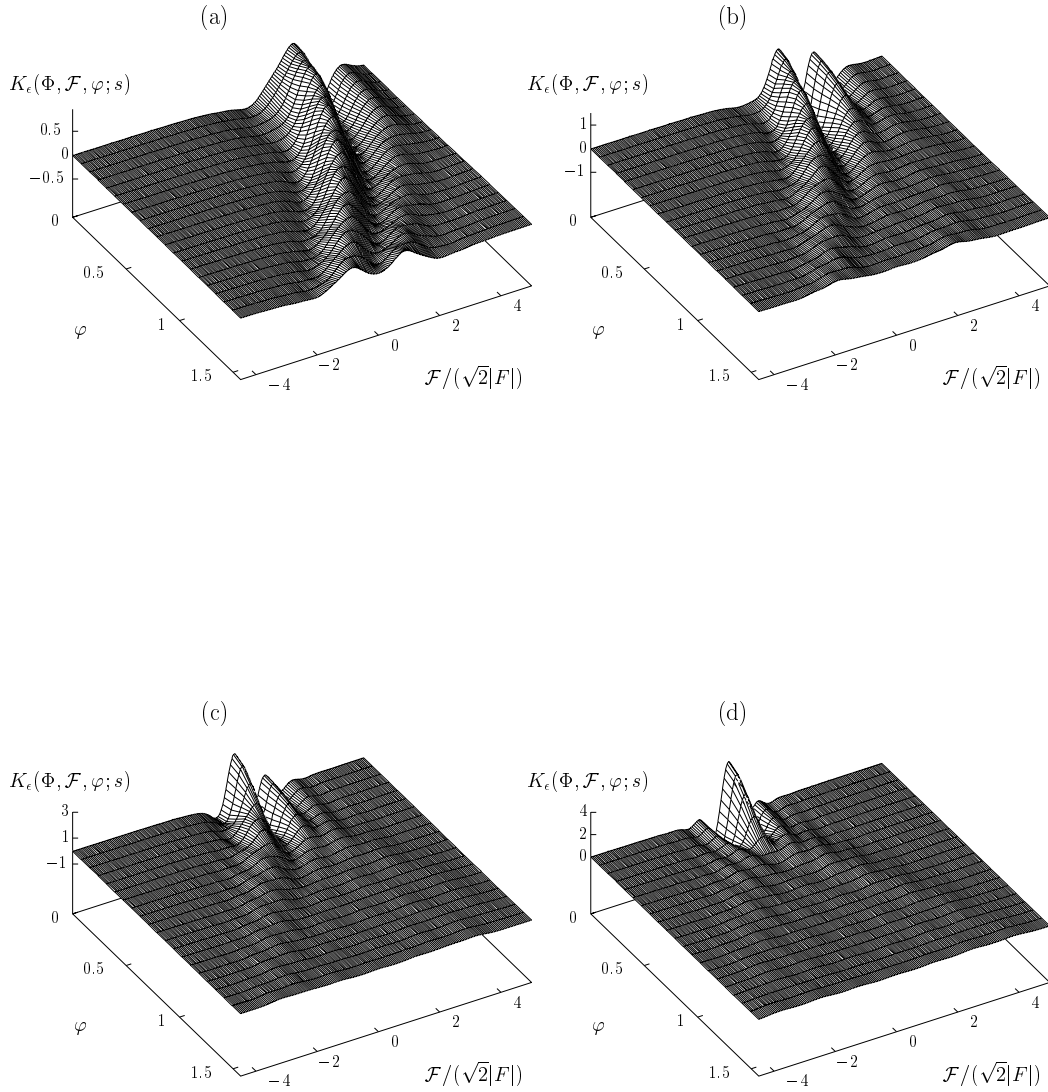


Figure 3: The dependence on \mathcal{F} and φ of the sampling function $K_\epsilon(\Phi, \mathcal{F}, \varphi; s)$ is shown for various values of Φ , the values of s and ϵ being $s = 0$ (perfect detection) and $\epsilon = 0.4$; $\Phi = \frac{1}{8}\pi$ (a), $\Phi = \frac{1}{4}\pi$ (b), $\Phi = \frac{3}{8}\pi$ (c), $\Phi = \frac{1}{2}\pi$ (d).

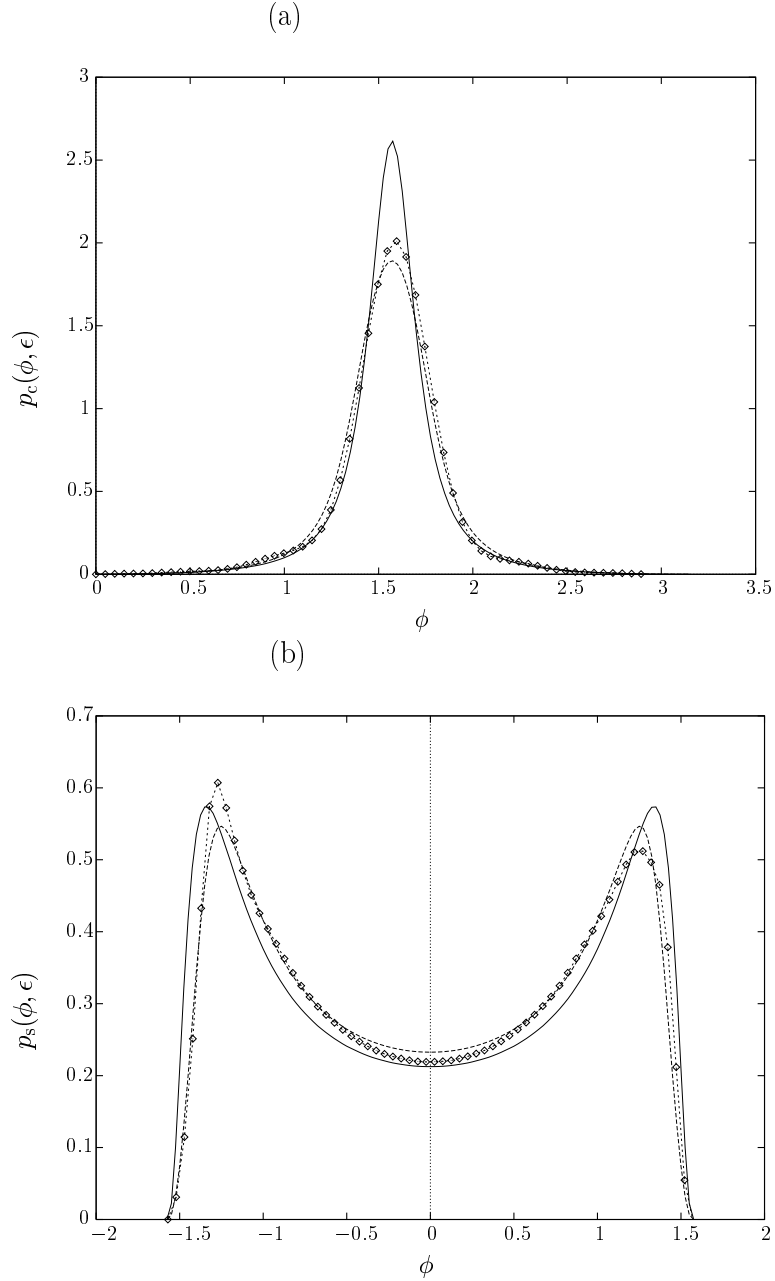


Figure 4: The measured Susskind–Glogower cosine (a) and sine (b) phase state distributions (double dotted lines) of a signal mode prepared in a squeezed vacuum state, Eq. (43), with mean photon number $\langle \hat{n} \rangle = 1$ ($\xi = 0.88$) are compared with the calculated distributions (dashed lines), the values of s and ϵ being $s = 0$ (perfect detection) and $\epsilon = 0.4$. The solid lines represent the exact distributions that are observed in the limit $\epsilon \rightarrow 0$. In the computer simulation of measurements $10^4 \times 30$ events (30 phase values) are assumed to be recorded.